DESIGN OF A PHOSWICH WELL DETECTOR FOR RADIOXENON MONITORING

W. Hennig[1], H. Tan[1], A. Fallu-Labruyere[1], W. K. Warburton[1], J. I. McIntyre[2], A. Gleyzer[3]

XIA, LLC[1], Pacific Northwest National Laboratory[2], and PhotoPeak, Inc.[3]

Sponsored by National Nuclear Security Administration
Office of Nonproliferation Research and Development
Office of Defense Nuclear Nonproliferation

Contract No. DE-FG02-04ER84121[1,2,3]

ABSTRACT

The network of monitoring stations established through the Comprehensive Nuclear-Test-Ban Treaty includes systems to detect radioactive xenon released into the atmosphere from nuclear weapons testing. One such monitoring system is the Automated Radio-xenon Sampler/Analyzer (ARSA) developed at Pacific Northwest National Laboratory. For high sensitivity, the ARSA system currently uses a complex arrangement of separate beta and gamma detectors to detect beta-gamma coincidences from characteristic radioxenon isotopes in small samples of xenon extracted from large volumes of air. The coincidence measurement is very sensitive, but the large number of detectors and photomultiplier tubes requires careful calibration.

A simplified approach is to use a single phoswich detector, consisting of optically coupled plastic and CsI scintillators. In the phoswich detector, most beta particles are absorbed in the plastic scintillator and most gamma rays are absorbed in the CsI, and pulse shape analysis of the detector signal is used to detect coincidences. As only a single detector and electronics readout channel is used, the complexity of the system is greatly reduced. Previous studies with a planar detector have shown that the technique can clearly separate beta only, gamma only and coincidence events, does not degrade the energy resolution, and has an error rate for detecting coincidences of less than 0.1%.

In this paper, we will present the design of a phoswich well detector, consisting of a 1" diameter plastic cell enclosed in a 3" CsI crystal. Several variations of the well detector geometry have been studied using Monte Carlo modeling and evaluated for detection efficiency, effects on energy resolution, and ease of manufacturing. One prototype detector has been built and we will present here some preliminary experimental results characterizing the detector in terms of energy resolution and its ability to separate beta only, gamma only, and coincidence events.

OBJECTIVES

The network of monitoring stations established through the Comprehensive Nuclear-Test-Ban Treaty includes systems to detect radioactive xenon released into the atmosphere from nuclear weapons testing. One such monitoring system is the ARSA developed at Pacific Northwest National Laboratory (Reeder et al., 1998). The ARSA system consists of a pair of large NaI(Tl) scintillator crystals holding four cylindrical fast plastic scintillator (BC-404) cells which are optically isolated from the NaI(Tl). The cells are filled with the xenon gas to be counted, which decays by emitting gamma rays or X-rays in coincidence with beta particles or conversion electrons. The plastic scintillator is meant to absorb all beta particles and conversion electrons, while the longer range gamma rays and X-rays will mainly be absorbed in the NaI(Tl) scintillator. Each BC-404 cell and each NaI(Tl) crystal is coupled to a pair of photomultiplier tubes (PMTs) and is read out by independent electronic channels. The sensitivity for detecting xenon isotopes is greatly increased by requiring coincidence between the signals from the PMTs coupled to the NaI(Tl) and the signals from the PMTs coupled to the BC-404.

While obtaining high coincidence detection efficiency and resolutions of about 25% for characteristic 80keV gamma rays, the current ARSA system design is operationally complex. The principle of time based coincidence, while effective in suppressing the background, requires separate signals from the NaI(Tl) and the BC-404, i.e. separate PMTs and readout electronics. In particular, the 12 PMTs require careful gain matching and calibration, and as the PMT gains change with time, voltage and temperature, the system easily drifts out of calibration. A simplified approach is to use a single phoswich detector (Ely et al., 2003), in the most recent implementation consisting of optically coupled plastic and CsI(Tl) scintillators (Hennig et al., 2006). The plastic scintillator is meant to absorb all beta particles and conversion electrons, while the longer range gamma rays and X-rays are mainly absorbed in the CsI(Tl) scintillator. Beta-gamma coincidences are then detected using pulse shape analysis of the detector signal. As only a single detector and electronics readout channel is used, the complexity of the system is greatly reduced.

Previous studies with a small planar detector showed that the technique can clearly separate beta only, gamma only and coincidence events, does not degrade the energy resolution, and has an error rate for detecting coincidences of less than 0.1%. In this paper, we will present the design of a phoswich well detector, consisting of a 1" diameter plastic cell enclosed in a 3" CsI crystal.

RESEARCH ACCOMPLISHED

1. Geometry of Phoswich Well Detector

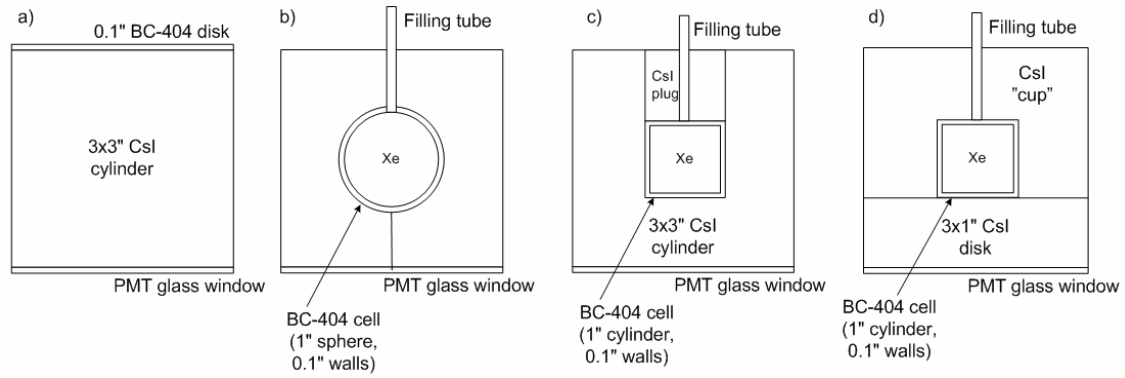

Figure 1. Geometries of detector designs studied. All outer surfaces have a diffuse reflective coating, all interfaces between CsI and BC-404 or CsI and CsI have optical couplant.

The geometry of the well detector has the following design constraints: i) to contain the volume of a typical radioxenon sample of 2-3 cm^3, the inner volume of the plastic cell should be 6-10 cm^3; ii) according to radiation transport simulations described in (Hennig, 2006), in order to stop all beta radiation but not absorb a significant amount of X-rays or gamma rays, the cell wall thickness should be 0.1"; iii) to absorb most of the X-rays and gamma rays, the cell must be surrounded by 1" of CsI on all sides. These constraints can be met with a variety of detector designs. The designs studied so far in detail are shown in Figure 1: a) a planar geometry, scaled up in size from the detector used in the previous work, b) a spherical cell with a vertical split, c) a cylindrical cell with a 1" plug, and d) a cylindrical cell with a horizontal split.

Figure 2 shows the results of Monte Carlo light collection simulations (using DETECT2000) for these geometries, assuming an index of refraction of 1.50 for the PMT glass window and the optical couplant, 1.58 for the BC-404 and 1.85 for the CsI. Variations in collection efficiency causes different amounts of light to be collected for gamma rays of the same incident energy interacting in different locations of the detector. Weighting the light collection efficiency data obtained in the simulation according to the volume each point represents (i.e. in first approximation, the probability of interaction), we obtain an estimate of the contribution of the crystal non-uniformity to the broadening of peaks in the energy spectrum. The probability distributions for each simulated detector are shown in Figure 3 and the peak resolutions range from 1.3% for geometry a) with a reflective constant of RC = 0.99 on the outer surface of the detector to double peaks with an overall ~6% width for geometry d) with RC = 0. 90, as listed in Table 1. This peak broadening due to light collection non-uniformity is only one contribution to the overall energy resolution of the detector, adding in quadrature to contributions from other effects such as photostatistics, crystal non-uniformities and energy non-linearities. In a good quality CsI detector, the overall energy resolution is typically ~17% for characteristic 80 keV gamma rays emitted from radioxenon. Therefore, as long as the changes in the light collection efficiency due to the embedded cell or the crystal geometry are minor, the energy resolution of the detector will not worsen significantly.

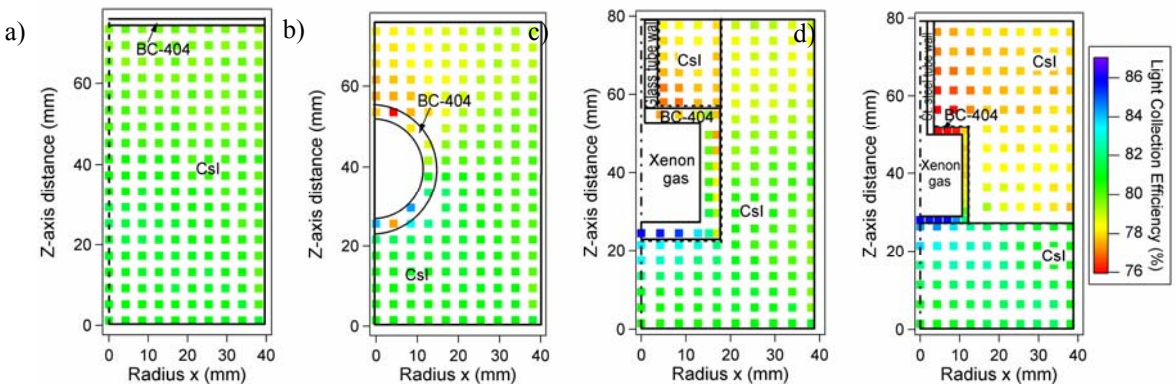

Figure 2. Geometric distribution of light collection efficiency for outer reflection coefficients = 0.95. By symmetry, only half of the crystal is simulated (from radius x=0 to 38mm).

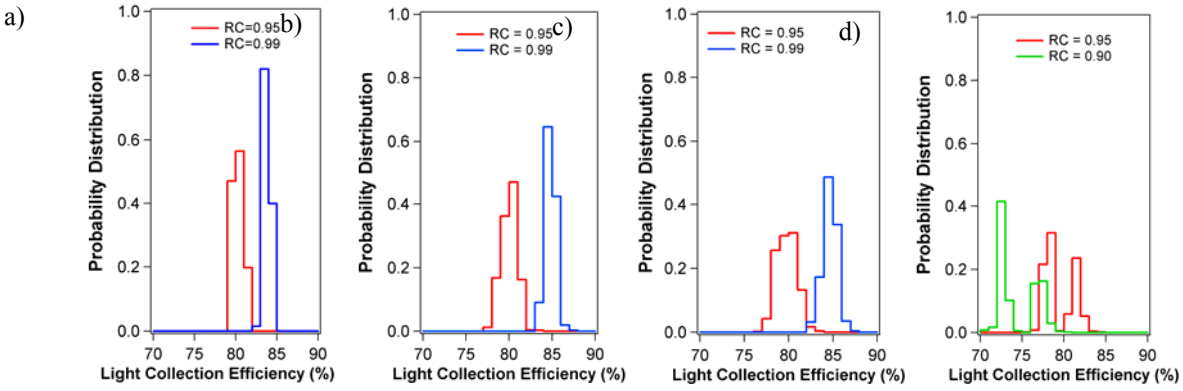

Figure 2. Volume-weighted distribution of light collection efficiency.

Table 1. Resolution due to non-uniformity of light collection for the detector geometries studied, with various values for the reflective constant RC on the outer surface of the detector

	Resolution (RC = 0.99)	Resolution (RC = 0.95)	Resolution (RC = 0.90)
Detector a)	1.3%	2.4%	--
Detector b)	1.8%	2.9%	--
Detector c)	2.3%	3.8%	--
Detector d)	--	~5%	~6%

The detection efficiency for beta-gamma coincidences in geometry a) is poor since a source in front of the detector will emit at least half of the beta particles and half of the gamma rays or X-rays away from the detector and thus at most 25% of coincidences will be detected. This geometry, used on a smaller scale in the previous work to study the principle of the phoswich detector and pulse shape analysis, here serves only as a comparison for the other geometries. In all geometries b) – d), the thickness of the plastic cell is the same and differences in cell geometry are minor which means that beta particles and conversion electrons have the same probability to be detected. The shape of the surrounding CsI varies somewhat in the different geometries. However, in each geometry there is at least 1″ of CsI in any direction of the plastic cell, absorbing 88 % of the highest energy gamma rays (~250 keV) and 99% or more for X-rays and gamma rays up to 164 keV. In some directions the radiation will have to travel through more CsI before escaping the detector and thus have a higher chance to be fully absorbed. For example, radiation emitted at the center of the detector towards the corner of the outer cylinder will travel through up to 1.41" of CsI in geometries c) and d), but 1.62" in geometry b). However, the increase in absorption efficiency is relatively small (e.g. to 95% for 1.5" of CsI for 250 keV), lower energy gamma rays are almost fully absorbed in 1″ already, and the variations between the geometries b) to d) are minor. Therefore, we can also assume the probability to absorb and detect X-rays and gamma rays to be essentially equal. Thus for geometries b) – d), the coincidence detection efficiency is the same as estimated in (Hennig, 2006); it is between 82% and 92% for the various radioxenon isotopes.

A further concern is ease of manufacturing. While geometry a) is a commonly used shape and easy to manufacture, geometries b) – d) require custom machining of the CsI; especially challenging for geometry b). In addition, during assembly of the well detector, it is important not to trap any air at the interfaces of the CsI and the plastic cell which will obstruct the light collection. For planar surfaces within the detector, such as the interface below the plastic cell in geometry c), trapping of air is in practice almost impossible to avoid.

Therefore, even though geometry d) has the highest non-uniformity of light collection, it was considered the easiest to manufacture and assemble, and was subsequently built as the first prototype of the well detector. Since for a given geometry, the two key parameters that increase uniformity of light collection are the outer reflectivity and the index of refraction of the optical couplant, care was taken during manufacturing to make them at least equal to 0.95 and 1.50, respectively. Experiments are under way to quantify the penalties associated with the less uniform light collection of design d) and additional geometries are being studied for future prototypes.

2. Measurements with Prototype Well Detector

The prototype detector (geometry d) was tested first with a weak ^{137}Cs needle source inserted into the detector through the filling tube, second with a stronger external ^{137}Cs source, and third with Xe gas sources at PNNL. The ^{222}Rn source was placed into a container connected to the filling tube and the ^{222}Rn gas gradually diffused into the detector. The PMT was read out with a DGF Pixie-4 (Hennig, 2005) that also calculated filter sums for further offline analysis as described previously (Hennig, 2006). In the analysis, pulses were categorized as 1) CsI only, 2) plastic only, and 3) combination pulses (see Figure 4) and their energy contributions in each part of the detector were calculated.

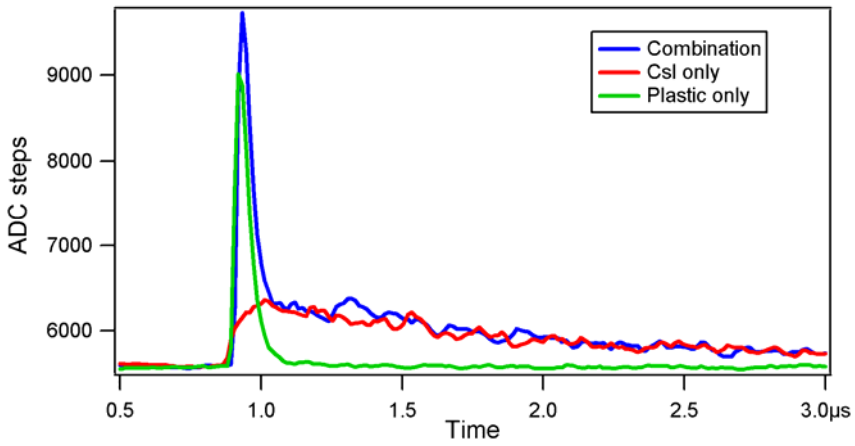

Figure 4. Pulse waveforms from the phoswich well detector.

In the small planar phoswich detector in the previous work, we measured a resolution of ~7% at 662 keV, a typical value for high quality CsI. For the well detector, using the external source, we measured between 11.5% and 12.8% resolution depending on the position of the source (see Figure 5). In addition, the peak position shifted by about 6.8% from the measurement with the source at the front to the measurement with the source at the back. The shift is expected from our light collection simulations, since the different source positions cause different parts of the detector to be irradiated, The measured value of 6.8%, though, is slightly higher than the 5-6% expected from the light collection simulations.

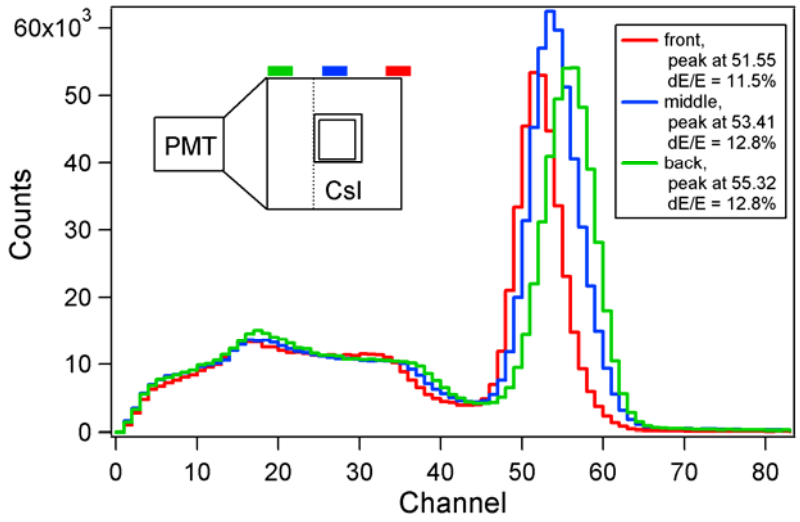

Figure 5. MCA spectra of ^{137}Cs source placed in various positions on the phoswich well detector. The output count rate was 12,000 – 14,000 cps.

With the ^{137}Cs needle source, the count rate is ~150 cps with lead shielding around the detector. The pulse shape analysis categorized ~53% of the events as CsI only, 41% as plastic only, and 2% as combination events. The resolution of the 662 keV peak for CsI only events is 12.8%. In the measurements with ^{137}Cs, there are no beta-gamma coincidences, but gamma rays are Compton scattered between CsI and the plastic scintillator, so the combination events form a line of constant energy in the scatter plot of energy deposited in the CsI vs energy deposited in the plastic (Figure 6).

To get a first estimate of the background rejection rate of the detector and pulse shape analysis (PSA) algorithms, we took a further measurement without sources. With the lead shield, the background rate is about 12 cps, of which 91.3% were categorized as CsI only, 0.4% as plastic only and 0.7% as combination events. The remaining ~7.7% of events could not be categorized. (Without lead shield, the background rate is ~127 cps.). Though some of the

combination events may come from contaminants inside the detector (e.g. the natural radon present in air) and thus be true beta-gamma coincidences, as a worst case estimate we assume all combination events to be false coincidences, for example external gamma rays interacting with both parts of the detector or events wrongly categorized by the PSA. Thus we obtain the upper limit of false beta-gamma coincidences to be 0.7%, which means the background rejection rate is at least 99.3%.

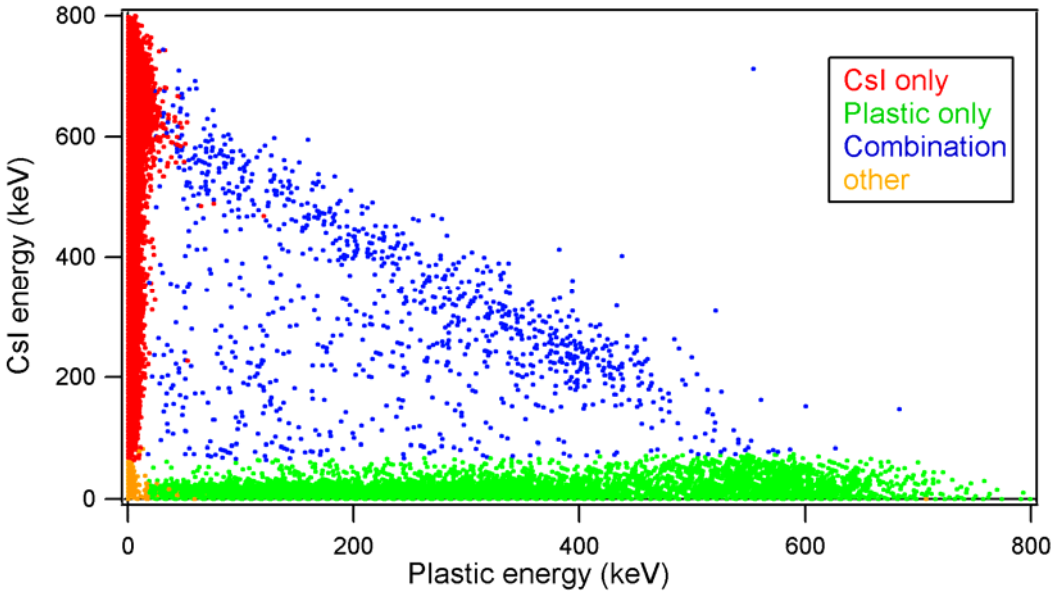

Figure 6. Two-dimensional energy scatter plot for ^{137}Cs. Note the diagonal line of constant total energy which is used for calibration of the plastic energy.

In the measurements with Xe sources at PNNL, the detector's filling tube was connected to a small pumping system. After background measurements, the cell was evacuated and filled with ^{131m}Xe. After several hours of data acquisition, the cell was evacuated again and flushed with air several times, later filled with ^{135}Xe for further measurements.

Fig. 7 shows a 2D energy scatter plot from measurements with ^{131m}Xe. Since ^{131m}Xe emits a conversion electron (with a fixed energy) in coincidence with an X-ray, the detector acquired a large number of combination events corresponding to beta-gamma coincidences. Most coincidence events fall into an area centered around 129keV plastic energy and 30keV CsI energy. Some conversion electrons loose a portion of their energy (e.g. due to absorption in the Xe itself) and thus fall in a band of varying plastic energy and a fixed CsI energy of 30keV. A second, weaker band is visible at ~80 keV, probably due to impurities from ^{222}Rn or ^{133}Xe. In some cases, conversion electron pass through the plastic cell and deposit part of their energy in the CsI, forming a diagonal band of events with constant overall energy.

CsI only events (not in coincidence with betas) fall on the vertical axis. Plastic only events (no coincidence with beta) fall on the horizontal axis and cluster at ~164 keV, corresponding to a non-coincident conversion electron emission from ^{131m}Xe.

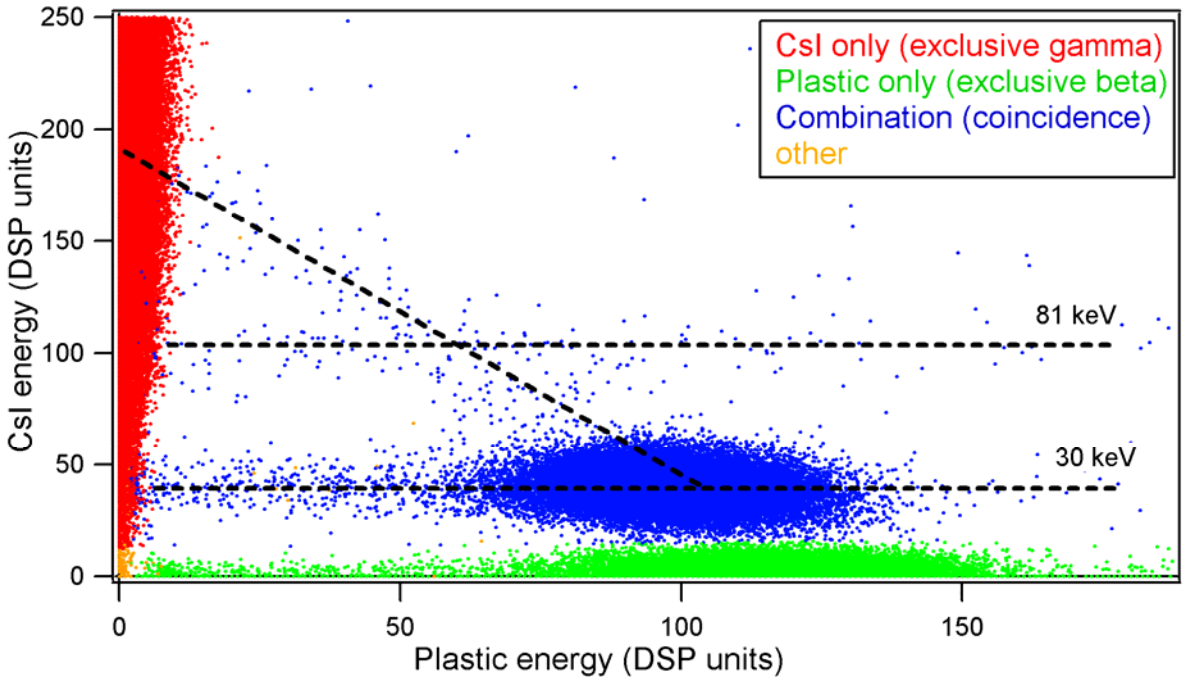

Figure 7. 2D energy scatter plot of events acquired with the phoswich well detector using a ^{131m}Xe source.

Figure 8 shows the spectra of energies deposited in the CsI (top, projection on vertical axis of Fig. 7) and the BC-404 (bottom, projection on horizontal axis). The resolution for the beta peaks is about 27%. Resolution for the 30 keV peak is about 45.8%, for the 81 keV peak about 29.6%. The 30 keV peak contains ~4.43×10^5 events in the histogram of all gammas and ~4.34×10^5 events in the histogram of coincident gammas (sum over peak minus background). Thus a first estimate for the coincidence detection efficiency at 30 keV is 97.9%.

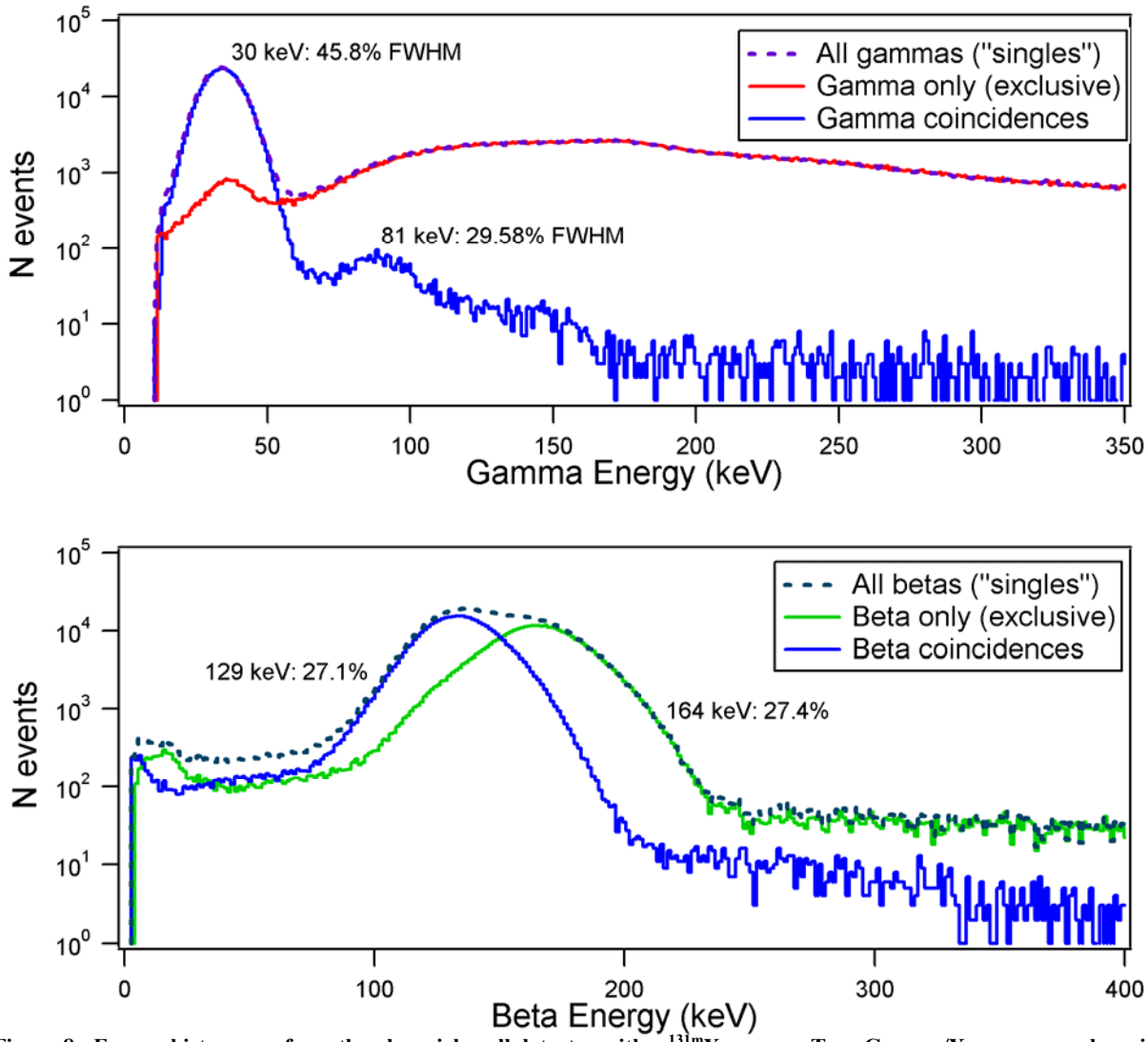

Figure 8: Energy histograms from the phoswich well detector with a ^{131m}Xe source. Top: Gamma/X-ray energy deposited in the CsI. Bottom: Beta energy deposited in the BC-404.

The ^{135}Xe source used in the later measurements at PNNL was much weaker than the previously used ^{131m}Xe source. Therefore the count rate and consequently the statistics are much lower in the ^{135}Xe measurements. In addition, some of the ^{131m}Xe remained trapped in the walls of the plastic cell (memory effect) and thus added a "background" of ^{131m}Xe events to the ^{135}Xe measurements. However, the band of combination events corresponding to coincidences of a 250 keV gamma with a beta particle of varying energy (max. 905 keV) is clearly visible (see Fig. 9). The resolution of the 250 keV peak in the gamma energy spectrum of coincidence events is about 17.6 % (see Figure 10).

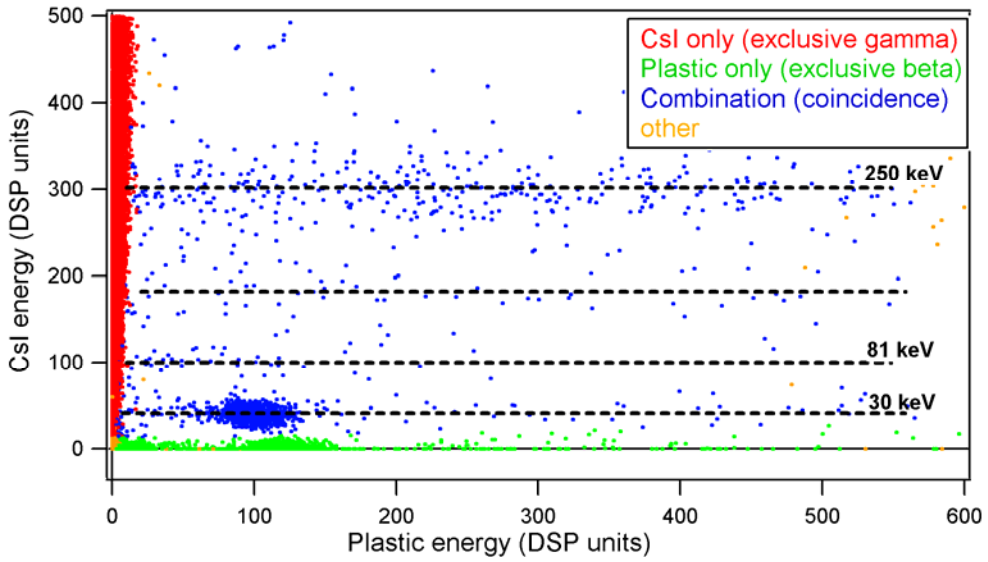

Figure 9: 2D energy scatter plot of events acquired with the phoswich well detector using a ^{135}Xe source. Some ^{131m}Xe from the previous measurement still remains due to the memory effect in the plastic cell.

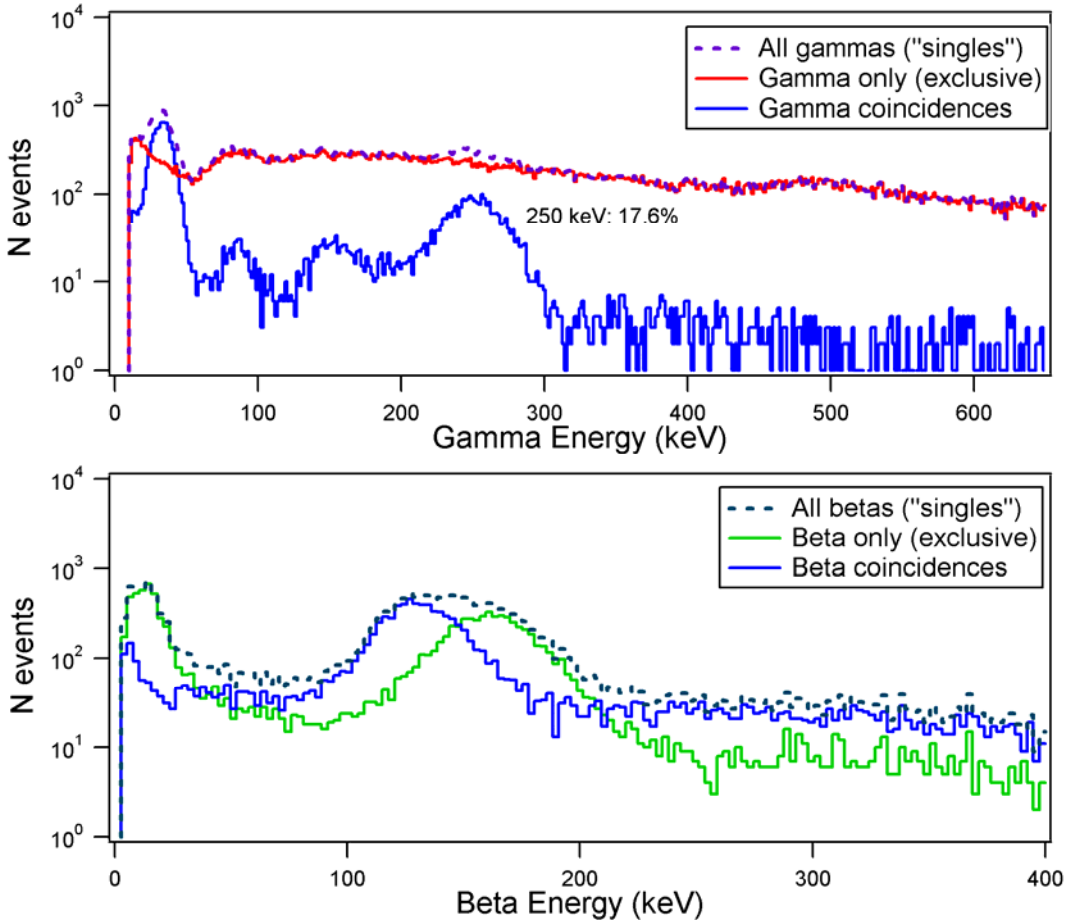

Figure 10: Energy histograms from the phoswich well detector with a ^{135}Xe source, but with some ^{131m}Xe remaining in the detector from the previous measurement. Top: Gamma/X-ray energy deposited in the CsI. Bottom: Beta energy deposited in the BC-404.

CONCLUSIONS AND RECOMMENDATIONS

In summary, a prototype phoswich well detector has been designed, modeled and manufactured. Preliminary test results using radioactive sources were presented. While the effects of crystal non-uniformity on the light collection in the detector and their possible limitations for the achievable energy resolution have to be studied further, preliminary measurements show that the detector is capable of detecting beta-gamma coincidences with high efficiency and separately measuring the energy deposited in each part of the detector. Further, as in our earlier work, the energy resolution of the CsI scintillator is not excessively degraded by application of the phoswich PSA algorithms. Work to date suggests that our models provide relatively accurate descriptions of phoswich detectors as built. The models, moreover, strongly suggest that it will be necessary to move toward a design more like geometry b), which has uninterrupted light paths between all parts of the CsI crystal and the PMT if we wish to achieve the highest energy resolution the technique is capable of. The prototype phoswich well detector will be used to further test the technology and to refine the PSA algorithms for better separation of event types. Our next goals are to develop a final detector design, based both on the geometry b) and on manufacturability issues, that will then be combined with designated readout electronics to create a replacement module for existing the ARSA detector and its readout electronics.

REFERENCES

Ely, J. H., C. E. Aalseth, J. C. Hayes, T. R. Heimbigner, J. I. McIntyre, H.S. Miley, M. E. Panisko, and M. Ripplinger (2003). Novel Beta-Gamma coincidence measurements using phoswich detectors, in *Proceedings of the 25th Seismic Research Review – Nuclear Explosion Monitoring: Building the Knowledge Base*, LA-UR-03-6029, Vol. 2, pp. 533–541.

Hennig, W., H.Tan, W. K. Warburton, and J. I. McIntyre, (2006). Single channel beta-gamma coincidence detection of radioactive Xenon using digital pulse shape analysis of phoswich detector signals, *IEEE Transactions on Nuclear Science* 53: (2) p. 620.

Hennig, W., Y.X. Chu, A. Fallu-Labruyere, W. K. Warburton, and R. Grzywacz, (2005). The DGF Pixie-4 spectrometer - compact digital read-out electronics for HPGe Clover detectors, presented at the IRRMA IV conference, Hamilton, ON, Canada, June 2005, submitted to *NIM B*.

Reeder, P. L., T.W. Bowyer, and R. W. Perkins, (1998). Beta-gamma counting system for Xe fission products, *Journal of Radioanalytical and Nuclear Chemistry*, 235: (1-2), 89–94.